Supplement to: JACC Cardiovascular Imaging 2020 (in press). Publisher DOI: 10.1016/j.jcmg.2020.02.028

Supplement

Shear stress estimated by quantitative coronary angiography predicts plaques prone to progress and cause events

Christos V. Bourantas,[a,b,c,#,*] MD, PhD; Thomas Zanchin,[a,d,e,#] MD; Ryo Torii,[e] PhD; Patrick W. Serruys,[f] MD, PhD; Alexios Karagiannis,[g] PhD; Anantharaman Ramasamy,[a,c] MBChB, MRCP; Hannah, Safi,[b] PhD; Ahmet Umit Coskun,[h] PhD; Gerhard Koning,[i] MSc; Yoshinobu Onuma,[j] MD, PhD; Christian Zanchin,[d] MD; Rob Krams,[k] MD, PhD; Anthony Mathur,[a,c] MD, PhD; Andreas Baumbach,[a,c] MD, FRCP; Gary Mintz,[l] MD; Stephan Windecker,[d] MD; Alexandra Lansky,[b,m] MD; Akiko Maehara,[l] MD; Peter H. Stone,[n] MD; Lorenz Raber,[d] MD, PhD; Gregg W. Stone,[m] MD

[a] Department of Cardiology, Barts Heart Centre, Barts Health NHS, London, UK

[b] Institute of Cardiovascular Sciences, University College London, London, UK

[c] Centre for Cardiovascular Medicine and Device Innovation, Queen Mary University London, London, UK

[d] Department of Cardiology, Bern University Hospital, Bern, Switzerland

[e] Department of Mechanical Engineering, University College London, London, UK

[f] Faculty of Medicine, National Heart & Lung Institute, Imperial College London, UK

[g] CTU Bern, Institute of Social and Preventive Medicine, Bern University, Bern, Switzerland

[h] Mechanical and Industrial Engineering, Northeastern University, Boston, MA

[i] Medis medical imaging systems bv, Leiden, The Netherlands

[j] Department of Interventional Cardiology, Thoraxcenter, Erasmus Medical Center, Rotterdam, the Netherlands

[k] Department of Molecular Bioengineering Engineering and Material Sciences, Queen Mary University London, London, UK

source: https://doi.org/10.7892/boris.144322 | downloaded: 25.4.2024

[l] Department of Cardiology, Columbia University Medical Center and the Cardiovascular Research Foundation, New York, NY

[m] Division of Cardiovascular Medicine, Department of Internal Medicine, Yale School of Medicine, New Haven, CT

[n] Cardiovascular Division, Brigham & Women's Hospital, Harvard Medical School, Boston, MA

Intravascular imaging analysis

VH-IVUS data analysis was performed by independent core-laboratories (Cardiovascular Research Foundation, New York, NY in PROSPECT and Cardialysis B.V., Rotterdam, The Netherlands in IBIS 4) using dedicated software (QCU-CMS, Medis, Leiden, the Netherlands for the PROSPECT and QIvus, Medis, Leiden, The Netherlands for the IBIS 4 study). In the PROSPECT study analysis was performed for the entire studied segment, while in IBIS 4 study analysis was performed only for the segment that was assessed by VH-IVUS at baseline and follow-up.

VH-IVUS segmentation in both core-laboratories was performed in every end-diastolic frame; in each frame the lumen, external elastic membrane (EEM), plaque area, plaque burden (PB) and its composition (i.e., fibrotic, fibrofatty, calcific and necrotic core area and burden) were estimated as previously described (1,2). Untreated VH-IVUS lesions were defined as ≥3 consecutive VH-IVUS frames visualizing segments with PB ≥40%. Lesion's remodeling pattern was calculated by the EEM area at the MLA divided by the average of the proximal and distal reference EEM area. Lesions with MLA and EEM area larger than the reference lumen and EEM area were considered to have excessive expanding remodeling; lesions with MLA smaller than the reference lumen area and EEM larger than the reference EEM area were assumed to have compensatory remodeling while, lesions with an EEM area smaller than the reference EEM area were considered to have constrictive remodeling (3). Classification of lesion phenotype was performed using the same protocol and methodologies described in a joint publication of the two core-laboratories (4). Based on its compositional traits, each lesion was classified as pathological intimal thickening (PIT), fibrotic, fibrocalcific, thick cap (ThCFA) and thin cap firboatheroma (TCFA) (4). ThCFA was defined as a lesion with a necrotic core component >10% in 3 consecutive frames; when the necrotic core was in contact with the lumen for 36^{o} along the lumen circumference the lesion was defined as TCFA.

To examine the inter-observer variability of the two core-laboratories in assessing plaque phenotypes 45 lesions (15 TCFA, 15 ThCFA and 15 PIT) were selected from the PROSEPCT study and were analysed from an expert analyst from Cardialysis B.V. who reviewed the VH-IVUS images and classified lesion phenotype. An excellent agreement was noted between Cardiovascular Research

Foundation and Cardialysis B.V. for all lesion types (κ=0.867, P<0.001): κ=0.951 for PIT (P<0.001), κ=0.806 for ThCFA (P<0.001) and κ=0.951 for TCFA (P<0.001).

Blood flow simulation and ESS estimation

Blood flow simulation was performed in the 3D-QCA models using proprietary software (ICEM 15.0 CFD and CFX 18.04, Ansys, Canonsburg, PA). To ensure a smooth transition and that the flow was fully developed when it entered into the reconstructed vessel, flow extensions – with a length equally to 15 diameters – were added in the inflow and outflow of the model, and in the final geometry blood flow simulation was performed. Blood was considered homogenous, Newtonian fluid with a density of 1,050 kg/m^3, while its viscosity was patient specific and estimated using the Walburn and Schneck equation (5). Although the Walburn-and-Schneck equation was established for non-Newtonian blood rheology, in our study blood features, as well as the mean shear rate calculated from the mean flow velocity and mean vessel radius were used as input parameters to calculate a "Newtonian version" of patient-specific viscosity. A flat flow profile was imposed at the inlet and zero pressure conditions at the outlet of each model. Blood flow was assumed to be steady, laminar and incompressible, the arterial wall was considered to be rigid and no-slip conditions were applied to the lumen surface. Blood flow was calculated by measuring the number of frames required for the contrast dye to pass through the segment of interest, the volume of the segment of interest and the cine frame rate (6,7).

References

1. Stone GW, Maehara A, Lansky AJ et al. A prospective natural-history study of coronary atherosclerosis. N Engl J Med 2011;364:226-35.
2. Raber L, Taniwaki M, Zaugg S et al. Effect of high-intensity statin therapy on atherosclerosis in non-infarct-related coronary arteries (IBIS-4): a serial intravascular ultrasonography study. Eur Heart J 2015;36:490-500.
3. Bourantas CV, Raber L, Sakellarios A et al. Utility of Multimodality Intravascular Imaging and the Local Hemodynamic Forces to Predict Atherosclerotic Disease Progression. JACC Cardiovasc Imaging 2019.
4. Garcia-Garcia HM, Mintz GS, Lerman A et al. Tissue characterisation using intravascular radiofrequency data analysis: recommendations for acquisition, analysis, interpretation and reporting. EuroIntervention 2009;5:177-89.
5. Wallburn F, Schneck D. A constitutive equation for whole human blood. Biorheology 1976;13:201-2018.
6. Coskun AU, Yeghiazarians Y, Kinlay S et al. Reproducibility of coronary lumen, plaque, and vessel wall reconstruction and of endothelial shear stress measurements in vivo in humans. Catheter Cardiovasc Interv 2003;60:67-78.
7. Stone PH, Saito S, Takahashi S et al. Prediction of progression of coronary artery disease and clinical outcomes using vascular profiling of endothelial shear stress and arterial plaque characteristics: the PREDICTION Study. Circulation 2012;126:172-81.

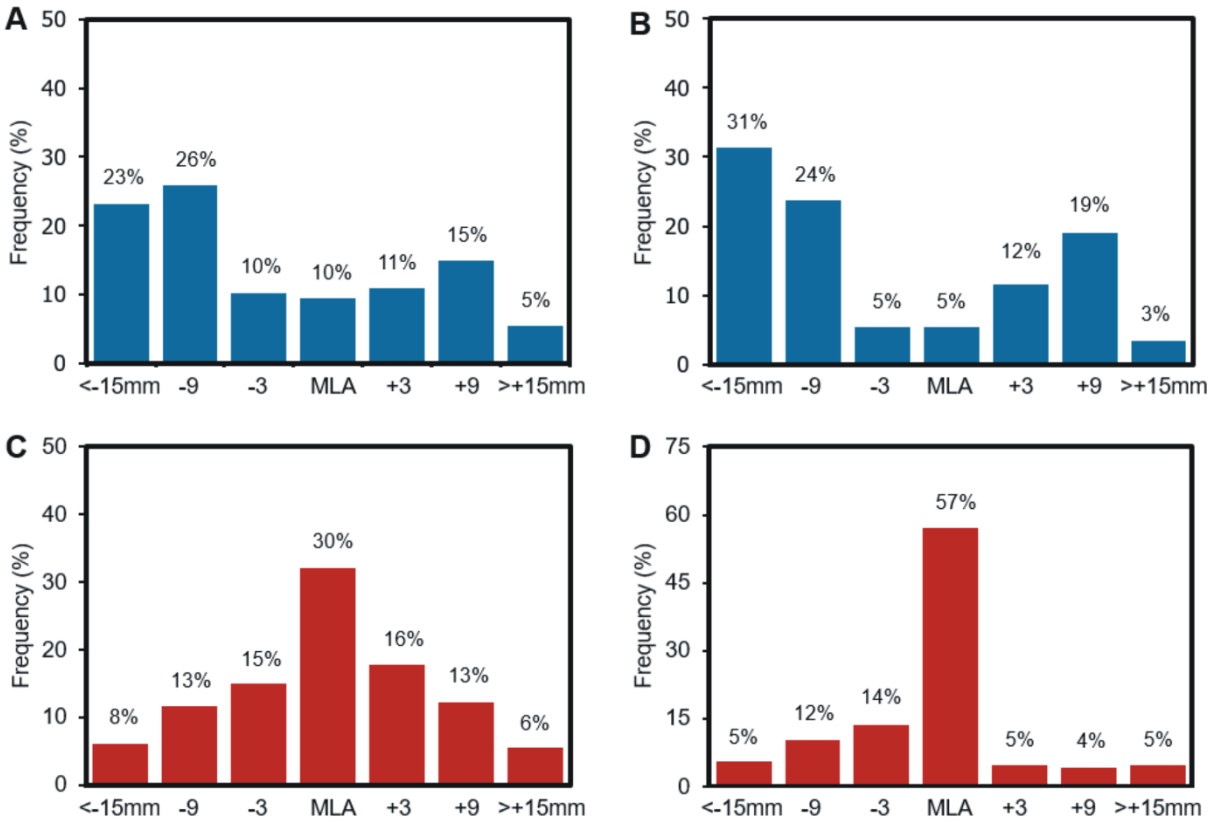

Supplementary Figure 1. Location of the minimum (A, B) and maximum (C, D) ESS values across the studied lipid-rich plaques. The MLA in panels (A, C) corresponds to the IVUS MLA while in panels (B, D) to the 3D-QCA MLA.

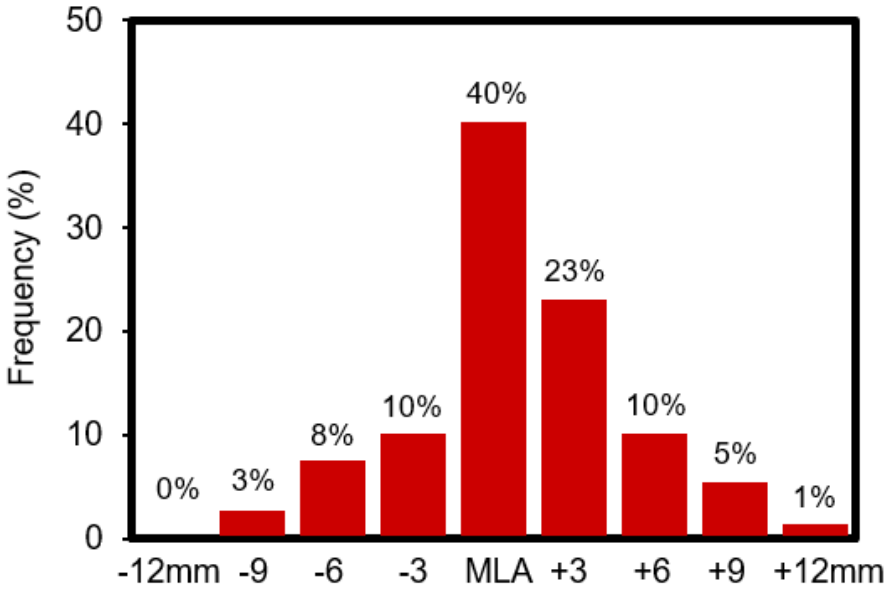

Supplementary Figure 2. Distribution of the QCA-derived MLA in relation to IVUS MLA (shown in the horizontal axis).

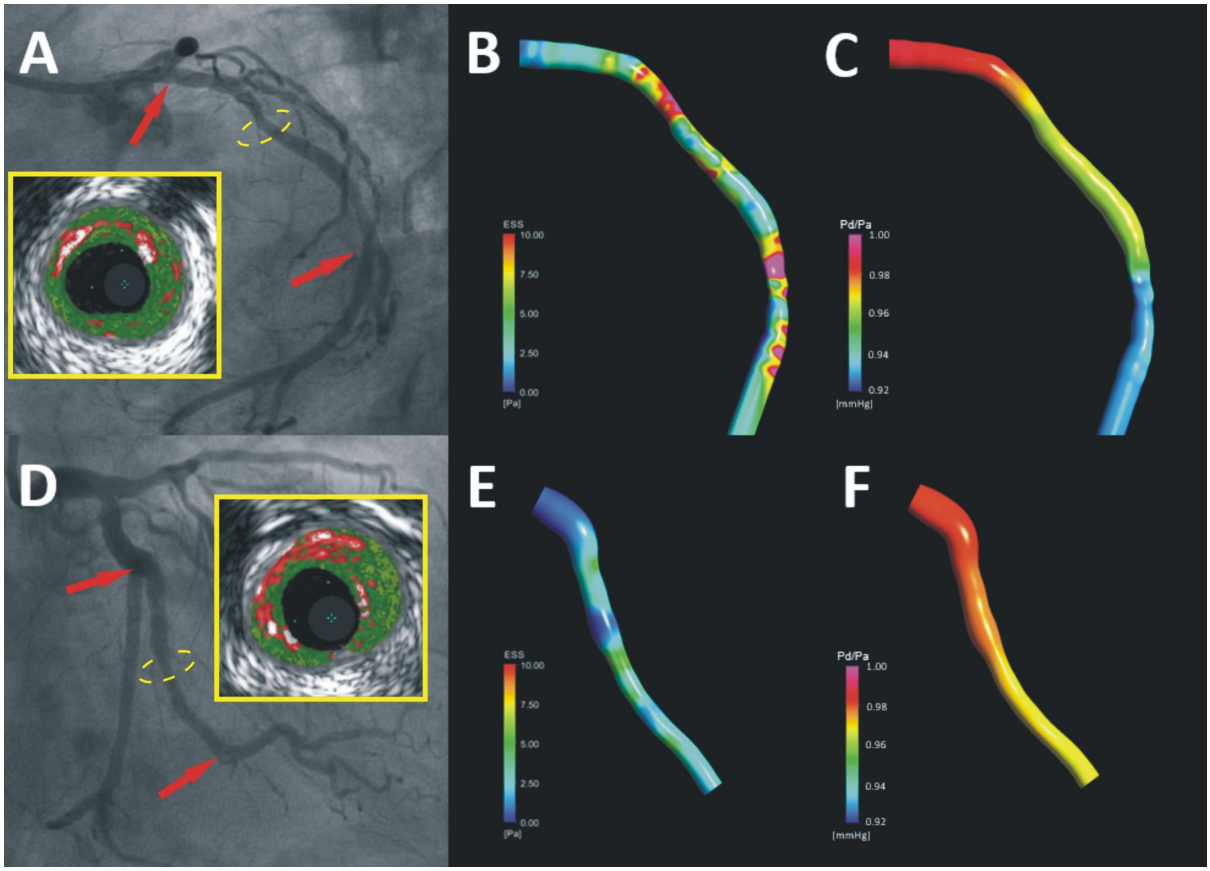

Supplementary Figure 3. A case example highlighting the value of 3D-QCA derived hemodynamic variables in predicting events. Panel (A) shows an angiographic projection of a lesion that caused a myocardial infarction at 6 months follow-up, while panel (D) the X-ray projection of a lesion that remained quiescent. The proximal and distal end of the reconstructed segments are shown with red arrows while the location of the MLA with a yellow dashed circle. As it is shown in the IVUS images (inset) there was no differences in the MLA (4.07mm^2 vs 3.73mm^2) and PB (72.2% vs 74.9%) between the two lesions, while the length of the lesion that caused myocardial infarction was shorter than the length of the lesion that remained quiescent (35.5mm vs 42.1mm). Conversely the maximum ESS (B, E) was significantly higher (7.86Pa vs 3.86Pa) and the pressure gradient (C, F) significantly lower (4.75mmHg vs 2.26mmHg) in the plaque that caused myocardial infarction than the plaque that remained quiescent.

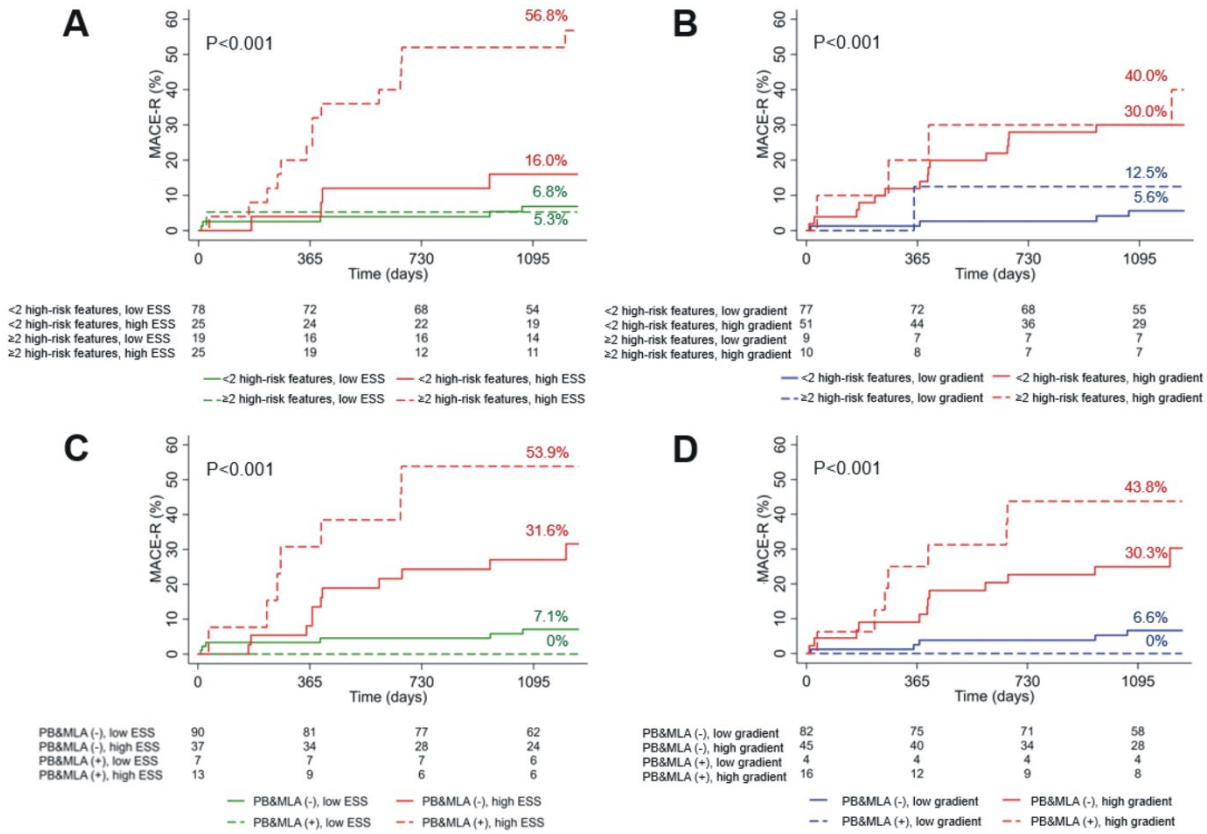

Supplementary Figure 4. Kaplan-Meier curves showing 3.4-year MACE-R rate according to plaque and 3D QCA-derived haemodynamic indices. Lesions were classified in groups according to the presence of absence of (A) ≥2 high-risk plaque features and increased maximum ESS values (>4.95Pa); (B) ≥2 high-risk plaque features and high pressure drop (<2.31mmHg) across the lesion; (C) PB ≥70%, MLA ≤4mm^2 and increased maximum ESS values and (D) PB ≥70%, MLA ≤4mm^2 and high pressure drop.

Supplementary Table 1. Baseline demographics of the patients recruited in the PROSPECT and IBIS 4 studies.

	Patients recruited in PROSPECT (N=45)	Patients recruited in IBIS 4 (N=47)	P
Age (years)	58.86 (55.0, 66.7)	55.90 (50.2, 64.7)	0.274
Gender (male)	38 (84%)	43 (92%)	0.299
BMI	26.8 (24.4, 30.1)	27.7 (24.5, 30.0)	0.953
Current smoker	22 (44%)	25 (49%)	0.613
Co-morbidities			
Diabetes mellitus	7 (16%)	8 (17%)	0.813
Hypertension	20 (44%)	22 (47%)	0.820
Hypercholesterolemia	16 (38%)	20 (43%)	0.669
Renal failure*	1 (3%)	2 (4%)	0.657
Previous PCI	5 (11%)	1 (2%)	0.081
Family history of CAD	18 (40%)	12 (26%)	0.139
Clinical presentation			**<0.001**
STEMI	11 (24%)	47 (100%)	
NSTEMI	30 (67%)	0 (0%)	
Unstable angina	4 (9%)	0 (0%)	
Medications at discharge			
Aspirin	44 (98%)	47 (100%)	0.304
Thienopyridines	45 (100%)	100 (100%)	-
Beta-blocker	42 (93%)	45 (96%)	0.610
RAAS inhibitor	30 (67%)	46 (98%)	<0.001
Statin	41 (91%)	47 (100%)	0.037

Table footnote: BMI, body mass index; CAD, coronary artery disease; PCI, percutaneous coronary intervention; NSTEMI, non ST-elevation myocardial infarction; RAAS, renin angiotensin aldosterone system; STEMI, ST-elevation myocardial infarction.

*Renal failure was defined as estimated glomerular filtration rate <60mL/min/1.73m^2.

Supplementary Table 2. Morphological and hemodynamic characteristics of the MACE and the non-MACE lesions.

	MACE lesions (N=22)	non-MACE lesions (N=125)	P
VH-IVUS plaque characteristics			
VH-IVUS lesion length (mm)	28.9 (16.2, 41.4)	20.9 (12.8, 33.8)	0.184
Distance vessel ostium to MLA (mm)	24.7 (14.5, 39.5)	24.2 (9.8, 35.0)	0.708
Length of the proximal shoulder (mm)	10.6 (5.5, 17.0)	11.6 (6.7, 23.4)	0.681
MLA (mm^2)	3.45 (3.24, 4.07)	5.01 (4.02, 6.60)	<0.001
EEM area (mm^2)	11.36 (10.33, 14.65)	13.71 (10.79, 16.53)	0.112
Plaque area (mm^2)	7.68 (7.00, 10.59)	7.96 (6.54, 10.62)	0.972
PB (%)	70.2 (65.3, 72.2)	61.1 (54.2, 66.5)	<0.001
TCFA phenotype	14 (63.6%)	83 (66.4%)	0.801
Remodeling pattern			0.210
Constrictive remodeling	13 (59.1%)	68 (54.4%)	
Compensatory remodeling	7 (31.8%)	54 (43.2%)	
Excessive expansive remodeling	2 (9.1%)	3 (2.4%)	
3D-QCA and CFD-derived variables			
3D-QCA lesion length (mm)	18.3 (14.1, 25.0)	17.4 (12.7, 25.3)	0.720
MLD (mm)	1.86 (1.52, 2.03)	2.22 (1.84, 2.53)	<0.001
Percentage DS (%)	36.5 (24.2, 44.0)	25.1 (20.3, 31.5)	0.005
Coronary blood flow (ml/s)	0.69 (0.55, 1.17)	0.90 (0.66, 1.17)	0.082
Maximum ESS value (Pa)	9.74 (6.46, 12.71)	4.73 (3.03, 6.99)	<0.001
Minimum ESS value (Pa)	1.44 (1.11, 1.99)	1.17 (0.78, 1.77)	0.083
Pressure drop across the lesion (mmHg)	3.90 (2.37, 5.62)	1.74 (0.99, 2.78)	<0.001
Lesion location			
Coronary artery			0.580

Left anterior descending artery	10 (39.5%)	48 (38.4%)	
Left circumflex artery	8 (36.4%)	36 (28.8%)	
Right coronary artery	4 (18.2%)	40 (32.0%)	
Intermediate coronary artery	0 (0%)	1 (0.8%)	
Coronary segment			0.790
Proximal vessel	14 (64%)	86 (69%)	
Mid vessel	4 (18%)	23 (18%)	
Distal vessel	4 (18%)	16 (13%)	

Table footnote: CFD, computational fluid dynamics.

Supplementary Table 3. Univariable and multivariable analyses of the morphological, angiographic and hemodynamic predictors of MACE-R (n=20) in lesions with a TCFA phenotype (n=97).

	Univariable analysis		Multivariable analysis*	
	Hazard ratio	**P**	**Hazard ratio**	**P**
MLA (per 1mm^2 increase)	0.53 (0.36, 0.79)	0.002	-	-
PB (per 1% increase)	1.11 (1.05, 1.18)	0.001	1.09 (1.02, 1.16)	0.008
MLD (per 1mm increase)	0.30 (0.11, 0.83)	0.020	-	-
Percentage DS (per 1% increase)	1.06 (1.01, 1.10)	0.009	1.02 (0.97, 1.07)	0.440
Maximum ESS value (per 1Pa increase)	1.20 (1.09, 1.33)	<0.001	1.14 (1.02, 1.29)	0.027
Pressure drop across a lesion (per 1mmHg increase)	1.23 (1.04, 1.46)	0.017	-	-

* Significant correlation (r>0.5) was noted between the maximum ESS and the MLA (r=-0.528, P<0.001), the MLD (r=-0.522, P<0.001) and the pressure drop across the lesion (r=-0.700, P<0.001). Maximum ESS was entered in the multivariate model as this variable had the highest area under the curve (AUC) in the receiver-operating characteristics analysis (AUC_{maxESS} = 0.795, P<0.001; AUC_{MLA} = 0.768, P<0.001; AUC_{MLD} = 0.693, P=0.009; $AUC_{pres\ drop}$ = 0.730, P=0.002).

Supplementary Table 4. Patient level univariable analyses of the morphological, angiographic and hemodynamic predictors of MACE-R (n=22).*

	Univariable analysis**	
	Hazard ratio	**P**
MLA (per 1mm^2 increase)	0.53 (0.35, 0.80)	0.002
PB (per 1% increase)	1.10 (1.04, 1.17)	0.002
MLD (per 1mm increase)	0.20 (0.07, 0.62)	0.005
Percentage DS (per 1% increase)	1.06 (1.02, 1.11)	0.005
Maximum ESS value (per 1Pa increase)	1.11 (1.05, 1.18)	0.001

* In patients with multiple lesions the lesion with the highest maximum ESS value was entered into the model.

** Significant correlation (r>0.5) was noted between the maximum ESS and the MLA (r=-0.575, P<0.001). Considering the large number of predictors and the relative small number of events reported multivariable Cox regression analysis was not performed.